



Chemical explosion, COVID-19, and environmental justice: Insights from low-cost air quality sensors

Guning Liu^a, Katie Moore^{b,c}, Wei-Chung Su^{a,d}, George L. Delclos^{a,d}, David Gimeno Ruiz de Porras^{a,d}, Bing Yu^a, Hezhong Tian^e, Bin Luo^f, Shao Lin^g, Grace Tee Lewis^c, Elena Craft^c, Kai Zhang^{g,*}

^a Department of Epidemiology, Human Genetics and Environmental Sciences, The University of Texas Health Science Center at Houston School of Public Health, Houston, TX 77030, USA

^b Clarity Movement Co., Durham, NC, USA

^c Environmental Defense Fund, 301 Congress Avenue, Austin, TX, USA

^d Southwest Center for Occupational and Environmental Health, The University of Texas Health Science Center at Houston (UTHealth) School of Public Health, Houston, TX 77030, USA

^e State Key Joint Laboratory of Environmental Simulation & Pollution Control, School of Environment, Beijing Normal University, Beijing 100875, China

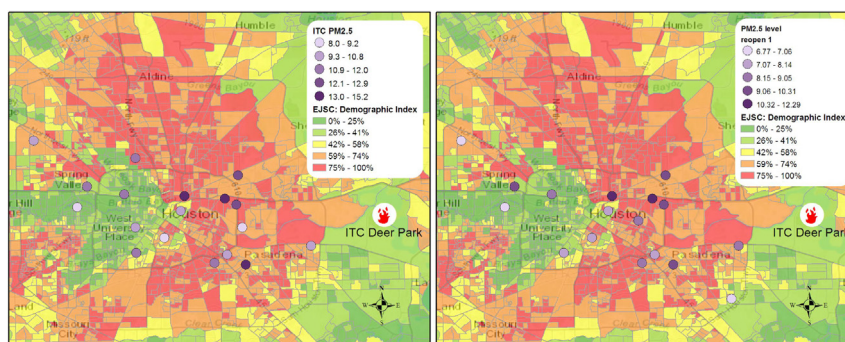
^f Institute of Occupational Health and Environmental Health, School of Public Health, Lanzhou University, Lanzhou, Gansu 730000, China

^g Department of Environmental Health Sciences, School of Public Health, University at Albany, State University of New York, Albany, NY, USA

HIGHLIGHTS

- First to study the impact of the chemical explosion on air quality with sensors
- The chemical explosion disproportionately affected disadvantaged communities.
- PM levels vary with COVID policies.
- Low-cost sensor networks provide high spatiotemporal variability.

GRAPHICAL ABSTRACT



ARTICLE INFO

Editor: Pavlos Kassomenos

Keywords:

Low-cost sensor
Particulate matter
Environmental justice
Industrial fire accident
COVID-19
Disaster
Air quality monitoring

ABSTRACT

Objectives: To examine the impact of the Intercontinental Terminals Company (ITC) fire and COVID-19 on airborne particulate matter (PM) concentrations and the PM disproportionately affecting communities in Houston using low-cost sensors.

Methods: We compared measurements from a network of low-cost sensors with a separate network of monitors from the Environmental Protection Agency (EPA) in the Houston metropolitan area from Mar 18, 2019, to Dec 31, 2020. Further, we examined the associations between neighborhood-level sociodemographic status and air pollution patterns by linking the low-cost sensor data to EPA environmental justice screening and mapping systems.

Findings: We found increased PM levels during ITC fire and pre-COVID-19, and lower PM levels after the COVID-19 lockdown, comparable to observations from the regulatory monitors, with higher variations and a greater number of locations with high PM levels detected. In addition, the environmental justice analysis showed positive associations between higher PM levels and the percentage of minority, low-income population, and demographic index.

Implication: Our study indicates that low-cost sensors provide pollutant measures with higher spatial variations and a better ability to identify hot spots and high peak concentrations. These advantages provide critical information for disaster response and environmental justice studies.

Synopsis: We used measurements from a low-cost sensor network for air pollution monitoring and environmental justice analysis to examine the impact of anthropogenic and natural disasters.

* Corresponding author at: Department of Environmental Health Sciences, School of Public Health, University at Albany, State University of New York, Albany, NY 12144, USA.
E-mail address: kzhang9@albany.edu (K. Zhang).

1. Introduction

Houston, TX, is one of the cities with significant air pollution health risks in the United States (US) due to its metropolitan population and industrialization. Particulate matter (PM), one type of air pollution commonly present in the ambient air (American Lung Association, n.d.; United States, n.d.), considerably impacts human health (American Lung Association, n.d.; United States, n.d.). The World Health Organization (WHO) estimated that, in 2016, PM from ambient air pollution contributed to 4.2 million premature deaths annually worldwide and 77,550 deaths in the U.S. (World Health Organization, n.d.) PM is associated with multiple health outcomes, including cardiovascular disease (Brook et al., 2010), respiratory disease (Hao et al., 2015; Krall et al., 2017), neurological disease (Younan et al., 2020), and mortality (Liu and Zhang, 2015). PM₁ (aerosol particulate matter with a median aerodynamic diameter $\leq 1 \mu\text{m}$) represent a subtype of PM that is more likely to penetrate the lower respiratory regions than larger size fractions of PM, such as PM₁₀ (diameter $\leq 10 \mu\text{m}$) (California Resources Board), and has been associated with stroke, dementia, Alzheimer's disease, and autism in a recent systematic review (Fu et al., 2019). Other PM size fractions, including PM₁₀ and PM_{2.5}, have also been reported to associate with respiratory diseases such as asthma, and cardiovascular disease, including myocardial infarction (Yang et al., 2018).

Air quality in the US is typically monitored by regulatory monitoring networks at the federal and state levels. These networks are systematically managed, yet, do not provide adequate exposure data for health-related research. Thus, some of the regulatory monitoring data are not ideal for assessing population exposures since monitors are limited in the number of pollutants they measured. And because monitors might not be where most civilian activity occurs, this creates a bias for ecological research. Second, expanding the monitoring areas and the range of pollutants is possible, yet quite expensive if done under a traditional regulatory monitoring network. But the expansion of monitoring can be less daunting and more affordable with the implementation of low-cost sensor networks that can significantly help capture more accurate air pollution data for health research without greatly increasing monitoring costs. The application of a low-cost sensor network has been carried out in several communities in California, finding that low-cost sensor networks can identify under-reported pollution and provide more details when mapping pollution over smaller areas. Several communities in California have taken this route (English et al., 2020). For example, in a 4-year observation comparison, English et al. found monitor variability was higher among low-cost sensors than regulatory monitoring data, which indicated low-cost sensor observations could more accurately reflect the distribution of pollution in the communities (English et al., 2020). A more recent study found a decrease in outdoor PM_{2.5} concentration and an increase in indoor PM_{2.5} concentration during the urban COVID-19 lockdown in California (Mousavi and Wu, 2021).

On March 17th, 2019, an industrial fire accident ignited at the Intercontinental Terminals Company (ITC) Deer Park facility in Houston, TX. The fire began at one of the facility's storage tanks, which contained naphtha. It then spread to other nearby tanks over the next six days (Deer Park Emergency Services, 2019). Part of the safety containment wall was destroyed in the process, leading to a major chemical leak into the Tucker Bayou and Houston Ship Channel, along with the water used to fight the fire. Local environment protection agencies and university research teams conducted air pollution sampling and analysis in and around the incident area to evaluate the aftermath of the ITC fire. These analyses showed increased levels of PM, black carbon, and volatile organic compounds during and shortly after the fire (Han et al., 2020; Texas Commission on Environmental Quality, 2020). However, to what extent and how this fire affected local communities still remains unclear because of the limited measurements during a short time period in previous studies. Additionally, while regulatory monitors provide critical information for decision-makers, they have several disadvantages, including a limited number of available sensors and higher maintenance costs. This study was designed

to fill this gap by implementing a low-cost sensor network that consists of air quality sensors with high deployment density and low cost.

In early 2020, soon after COVID-19 was declared a pandemic by the WHO, reports from Asia, Europe, and North America suggested a steep decline in air pollutant concentrations compared to the same time in 2019 (Berman and Ebisu, 2020; Patel, 2020; European Environment Agency, 2020; Bechle et al., 2013; Gautam, 2020). However, publications on associations between air pollution and a temporary decline in human activities during COVID-19 were inconclusive. A recent study found that the decreased traffic flow during COVID-19 lockdown in Italy was associated with the decrease in nitrogen oxides (Rossi et al., 2020). Another study from China suggested that even though biomass burning emission was reduced during COVID-19 lockdown, there was no association between reduced human activity and air pollution when adjusting for meteorological data (Wang et al., 2020). Therefore, there is still a need for research examining how air quality is affected by dramatic changes in human behavior related to industrial accidents (e.g., ITC fire) or pandemics (e.g., COVID-19). This research will provide important clues regarding air pollution control.

In this study, we will, first, present the data collected from low-cost sensor networks during the ITC fire incident and COVID-19 in Houston, TX; second, compare sensor data with regulatory monitoring data from the Environment Protection Agency (EPA) to examine the reliability of low-cost sensor networks and the impact of major accidents and anthropogenic behavior changes on air pollution levels; third, examine the association between low-cost sensor monitors observations and environment justice factors.

2. Methods

2.1. Sampling using low-cost sensor

2.1.1. Sensor operation principle

The Clarity Node-S (Clarity Movement Co., Berkeley, CA) is a low-cost sensor (LCS) that provides near-real-time data for PM, nitrogen dioxide, internal temperature, and relative humidity. The Node-S includes a laser particle counter (Plantower PMS6003) that operates using light scattering to generate an electrical signal converted to mass and number concentration measurements for 3 PM size cuts (PM₁, PM_{2.5}, PM₁₀). The Node-S sampling interval comprises three stages: a 90 s sample period, followed by a one- to two-minute upload period where the device transmits the measurement data to a data cloud, followed by a 15-min sleep period where the device powers off. The effective sampling frequency is the combined time of these three stages or about 17 to 19 min. The Clarity Node-S principle of operation has been described previously (Clarity, n.d.) and evaluated by AQ-SPEC (Air QSPECA-S, 2018a; Air QSPECA-S, 2018b), AirParif (Airparif-AirLab, 2018), and San Joaquin Valley Air Pollution Control District (SJVAPCD) (San JV-APCD, 2018).

2.1.2. Field deployment and instrument calibration

2.1.2.1. Data calibration and quality assurance. A regional Houston/Harris County PM_{2.5} correction model was developed using data from three Houston-area colocations (Supplementary Table 1). Based on hourly-averaged data from these three colocations, a multiple linear regression model (MLR) was developed using a random selection of 80 % of the hourly measurements for all sensors in the calibration group. Models using combinations of the following features were developed with 10-fold cross-validation repeated five times: PM₁, PM_{2.5}, and PM₁₀ mass concentration; PM₁, PM_{2.5}, and PM₁₀ number concentration; Temperature, Relative Humidity. The model with the highest R² was selected as the final Houston/Harris County regional model.

2.1.2.2. Measurements of air pollutants and weather parameters. The final regional model was applied to the hourly data for the complete set of 20 nodes to create a calibrated PM_{2.5} value (Supplementary Table 2).

Additional QA was done after calibration to remove data where the sensors may have been malfunctioning, including filtering data where relative humidity was >100 or below 0 % or when PM mass concentration was below -10 or above 2250 $\mu\text{g}/\text{m}^3$.

2.1.2.3. Site selection and characteristics. In March 2019, twenty Clarity Node-S devices were deployed in Harris County, TX, to monitor the air quality impacts of a chemical explosion and fire at the ITC chemical plant in Deer Park. Deployment of the network was done by City of Houston Health Department staff and employees of the non-profit Environmental Defense Fund (EDF) in collaboration with the Houston Fire Department. Nodes were concentrated on the east side of the city to capture impacts closest to the fire. Emphasis was placed on siting sensors within several neighborhoods of interest, especially those without existing regulatory monitors. Several sensors were placed in central and western Houston to measure potential changes in secondary PM formation. Devices were placed on rooftops of fire stations and private residences.

2.2. PM measurements at EPA monitors

Air pollution regulatory monitoring data were downloaded from the EPA Interactive Map of Air Quality System site (<https://www.epa.gov/outdoor-air-quality-data>). PM_{2.5} data were provided as daily averages from four monitors in the Houston area (Aldine, Houston east, Deer Park, and north loop). The first three monitors are reported daily, while the north loop sensor reports once every three days. PM₁₀ data were reported once every six days from five monitors in the Houston area (Clinton, Monroe, West hollow, Lang, and Texas city fire station). Meteorological data for the Houston area were collected from National Oceanic and Atmospheric Administration (NOAA) National Centers for Environmental Information (NCEI) (<https://www.ncdc.noaa.gov/cdo-web/datatools/lcd>).

2.3. Statistical analysis

To compare the data from low-cost sensors to EPA regulatory monitors, daily averages for each network were calculated. We used hourly average PM₁ and PM_{2.5} data from the twenty low-cost sensors to calculate daily averages. For PM₁₀, ten low-cost sensors' hourly data were included in the calculation. Based on ITC fire accident time and COVID case records and local regulations, we grouped the data into time ranges based on Harris County Judge and Texas Governor's Executive Orders (Table 1). We used a time-series plot to demonstrate the overall distribution of the data. To compare the network differences, we conducted two-sample *t*-test and F test with *p*-values of 0.05 considered statistically significant. We also calculated between (inter-) and within (intra-) monitor variance using maximum likelihood estimates for each pollutant and time range. Bland-Altman plots were used to examine the degree of agreement between the two networks. All computations were performed using R (version 4.0.5). We used ArcGIS to graphically examine the potential interaction between pollution distribution from the low-cost sensor network and environmental justice variables, including percentages of minorities, percentages of the low-income

population, percentages of low-education level populations, percentages of households in linguistic isolation, and demographic index which was the averaged sum of percent low-income and percent minority in each census block. Then we used linear regression to quantitatively examine the association of environmental justice variables with the statistical significance level of 0.05. Statistical analysis was completed using R (version 4.0.5), and geospatial analysis was completed using ArcGIS.

3. Results

3.1. Air quality results

After data calibration and quality assurance, we had 126,097 hourly observations on average from each low-cost sensor in the network for each pollutant, accounting for 656 days, which was the full length of our observation window. Regulatory data were provided in a daily format. PM_{2.5} had 656 observations, while PM₁₀ only had 134 observations ranging from March 22nd, 2019, to December 29th, 2020.

Fig. 1 shows the time series plots for the mean weekly concentrations for each pollutant from March 2019 to December 2020. For PM₁, concentrations were on average higher in winter months than in summer. For PM_{2.5}, observations were mostly consistent between low-cost sensors and regulatory monitors. Peak values were observed from both networks in Dec 2019 and July 2020. Only the low-cost sensor network had continuous observations for PM₁₀. The distribution of PM₁₀ concentration was similar to PM₁ with higher levels reported during winter.

Table 2 shows the descriptive analysis results and comparison of observations from each network in selected time periods. In general, the low-cost sensor network had a higher number of observations per day and less missing data.

Concentrations of PM₁, PM_{2.5} and PM₁₀ from low-cost sensors decreased one week after the ITC fire incident (Table 2). A similar trend was also found in the PM_{2.5} concentration from regulatory monitors. No statistically significant differences were observed between the two monitoring networks. Data showed comparable variability between low-cost and regulatory networks during the ITC fire incident and higher variability among low-cost sensors post-fire. Inter- and intra-monitor variances were similar between both networks.

The average level of PM₁ was higher pre-COVID than after, with slightly higher intra-variance in low-cost sensor observations (Table 2). Low-cost sensor data showed that levels of PM_{2.5} were slightly higher pre-COVID and during the lockdown, but such a difference was not observed from regulatory monitors. No statistically significant difference was found between PM_{2.5} levels between the two networks, except for the variance of average PM_{2.5} during COVID lockdown. The differences in PM₁₀ levels between the two networks were not consistent throughout the COVID-19 periods. Low-cost sensors detected higher levels of PM₁₀ pre-COVID compared to regulatory monitors with small data variability. The difference was statistically significant. When reopening first started (reopen stage 1: 5/1/2020–6/25/2020), low-cost sensors reported a significantly lower level of PM₁₀ with smaller variability, whereas, during the COVID winter wave came,

Table 1
Analysis time ranges based on Harris County and Texas COVID-19 policies.

Analysis period	Start date	Related policy	End date	Related policy
ITC fire	March 18th, 2019	start date of the incident	March 22nd, 2019	the last day with live fire
1-week post ITC fire	March 23rd, 2019	–	March 29th, 2019	–
pre-COVID	November 1st, 2019	Texas issued an executive state-wide order which limited social gathering to 10 people or less and closed all bars and restaurant	March 17th, 2020	Harris County closed all bars and restaurants
COVID lockdown	March 18th, 2020		June 10th, 2020	Harris County "Stay Home, Work Safe" order expired
COVID reopen stage-1	May 1st, 2020	Texas Stay-at-home executive order was lifted	June 25th, 2020	Texas paused further reopening followed by the re-shut down of all bars and limited restaurant activities
COVID reopen stage-2	September 23rd, 2020	1 week from Texas Executive Order 30 where business occupancy exemption was given in the order	December 31st, 2020	
COVID winter wave	November 11th, 2020	daily tested and hospitalization starts increasing rapidly	December 31st, 2020	

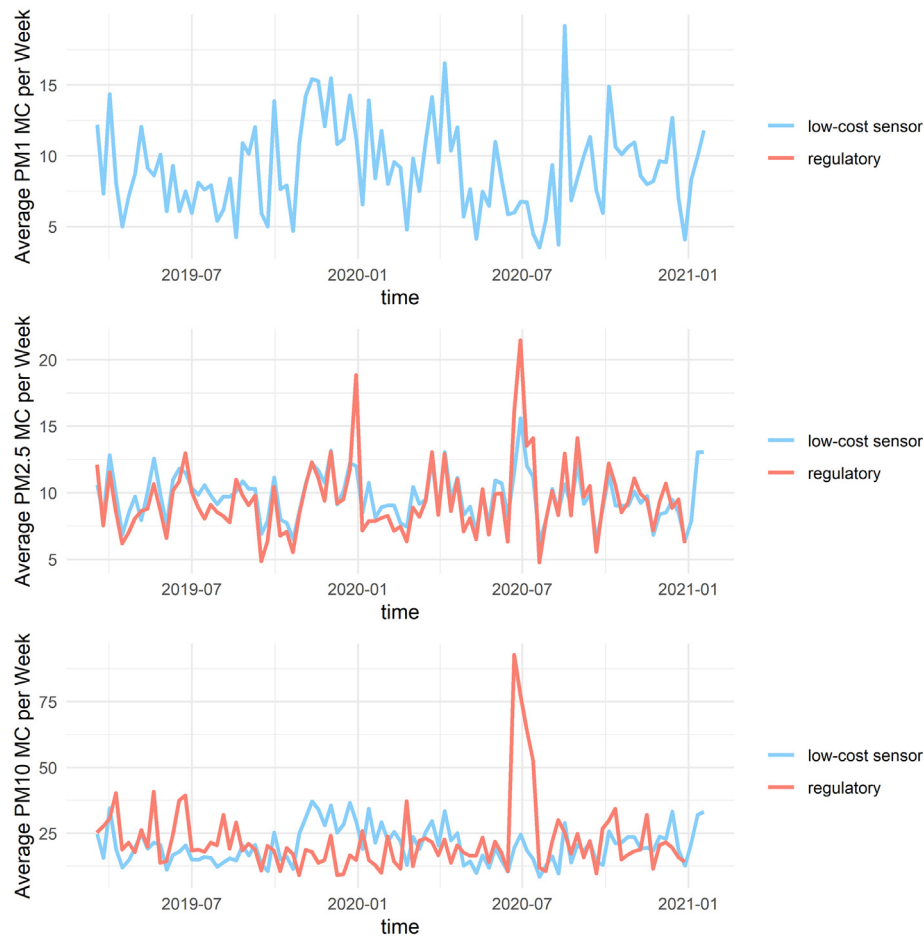


Fig. 1. Time series plots of PM_{2.5}, PM₁₀, and PM₁ weekly concentrations observed through EPA and low-cost sensor networks from March 18th, 2019 to December 31st, 2020.

Table 2

Low-cost sensor and regulatory network particulate matter averages, standard deviations, and t-test results.

		Low-cost sensor ^a						Regulatory						t-Test		Levene's test	
		N	Mean	SD	CV	Inter Variance	Intra Variance	N	Mean	SD	CV	Inter Variance	Intra Variance	t	p	F	p-value
PM ₁	ITC fire	73	11.12	1.87	16.9 %	−4.78	32.61	–	–	–	–	–	–	–	–	–	–
	1-week post fire	136	8.99	1.41	15.6 %	0.94	7.57	–	–	–	–	–	–	–	–	–	–
	pre-COVID	2425	11.08	1.32	11.9 %	1.52	43.04	–	–	–	–	–	–	–	–	–	–
	COVID lockdown	1431	9.70	0.96	9.9 %	0.52	39.39	–	–	–	–	–	–	–	–	–	–
	reopen stage 1	942	6.81	0.85	12.5 %	0.38	21.89	–	–	–	–	–	–	–	–	–	–
	reopen stage 2	1493	8.72	2.71	31.0 %	2.37	30.16	–	–	–	–	–	–	–	–	–	–
	COVID winter wave	757	8.72	1.50	17.2 %	1.71	33.33	–	–	–	–	–	–	–	–	–	–
PM _{2.5}	ITC fire	71	11.48	2.04	17.8 %	2.14	8.13	19	13.45	2.49	18.5 %	3.37	8.57	1.21	0.26	1.21	0.30
	1-week post fire	136	8.64	1.57	18.2 %	2.36	1.8	30	8.60	1.19	13.8 %	1.07	1.4	−0.08	0.94	1.28	0.28
	pre-COVID	2425	10.03	2.76	27.5 %	7.61	17.87	572	9.67	1.44	14.9 %	1.69	52.77	−0.58	0.56	1.26	0.26
	COVID lockdown	1432	9.82	1.87	19.0 %	3.58	12.99	362	9.37	1.44	15.3 %	0.89	14.23	−0.85	0.39	10.57	<0.01
	reopen stage 1	942	8.81	2.59	29.4 %	2.12	7.81	242	9.76	0.71	7.3 %	0.61	9.23	1.13	0.26	1.54	0.22
	reopen stage 2	1493	8.78	1.45	16.5 %	5.89	11.03	407	8.09	1.02	12.6 %	0.15	16.63	−1.34	0.18	3.70	0.06
	COVID winter wave	757	8.46	2.46	29.0 %	6.22	10.95	206	9.77	1.10	11.2 %	0.37	17.89	0.97	0.33	1.61	0.21
PM ₁₀	ITC fire	73	22.36	4.82	21.5 %	−13.87	146.27	–	–	–	–	–	–	–	–	–	–
	1-week post fire	136	18.00	3.63	20.2 %	10.53	20.19	–	–	–	–	–	–	–	–	–	–
	pre-COVID	2425	27.51	6.45	23.5 %	34.18	212.29	143	18.86	4.90	26.0 %	19.55	93.22	−3.18	<0.01	0.50	0.48
	COVID lockdown	1431	19.98	3.14	15.7 %	8.64	150.95	89	19.52	3.96	20.3 %	12.23	31.53	−0.23	0.81	12.80	<0.01
	reopen stage 1	942	13.25	2.47	18.7 %	5.54	56.59	56	17.25	3.75	21.7 %	10.35	31.41	2.26	0.03	12.98	<0.01
	reopen stage 2	1493	19.54	6.80	34.8 %	23.81	128.9	105	21.70	4.36	20.1 %	12.66	116.41	0.32	0.75	0.89	0.35
	COVID winter wave	757	21.39	5.02	23.5 %	23.08	173.36	55	18.69	3.46	18.5 %	5.05	62.41	−0.92	0.37	3.11	0.08

Time periods: ITC fire, 3/18/2019–3/22/2019; 1-week post fire, 3/23/2019–3/29/2019; pre-COVID, 11/1/2019–3/17/2020; COVID lockdown, 3/18/2020–6/10/2020; reopen stage 1, 5/1/2020–6/25/2020; COVID winter wave, 11/11/2020–12/31/2020; reopen stage 2, 9/23/2020–12/31/2020.

–, not enough data for calculation; N, number of days with available data; CV, coefficient variance; t, t-Test statistics; F, F-test statistics.

^a The minimum detection size for Optical Particle Counters used are 0.3 µg, thus ultrafine particles are not collected.

Table 3

Lin's concordance correlation coefficient (Rho) between low-cost sensors and regulatory network particulate matter daily averages during 2019–2020.

	Rho	95 % CI	b
PM _{2.5}	0.77	0.75–0.80	0.93
PM ₁₀	0.23	0.07–0.37	0.91

95 % CI: 95 % confidence interval; b: bias correction factor.

low-cost sensors reported a higher level of PM₁₀ with significantly greater variability.

We used the daily average data of each monitor from both networks to compare the data variance between (inter-) and within (intra-) their respective networks (Table 2). For both low-cost sensors and regulatory networks, the majority of the variance were from intra-monitor. Both inter-monitor variances were higher in the low-cost sensor network for PM_{2.5}, except

during the ITC fire period. Intra-monitor variances were mostly higher for the regulatory network. For PM₁₀, intra-monitor variances were higher for the low-cost sensor network, and inter-monitor variances were higher for low-cost sensors before COVID lockdown and after the reopening stage 1. Concordance coefficients showed a higher level of agreement for PM_{2.5} between the two networks, compared to PM₁₀ (Table 3).

Meteorology data from National Centers for Environmental Information (NCEI) showed the patterns of wind in Houston (Fig. 2). Winds in springs and summers were averagely 30 % of the time towards the southeast at 20 miles per hour (mph). In autumns and winters, the wind speed and direction varied between the year 2019 and 2020. In the first week after ITC fire, wind was mostly towards southeast at 21mph, while during the fire wind was multi-directional. During COVID-19 lockdown, 15 % of the time wind was southeasterly at 20 mph.

Bland-Altman plots (Fig. 3) showed a bias of -0.18 and an agreement range of -5.59 to 5.22 for PM_{2.5}, and a bias of 2.65 with the agreement

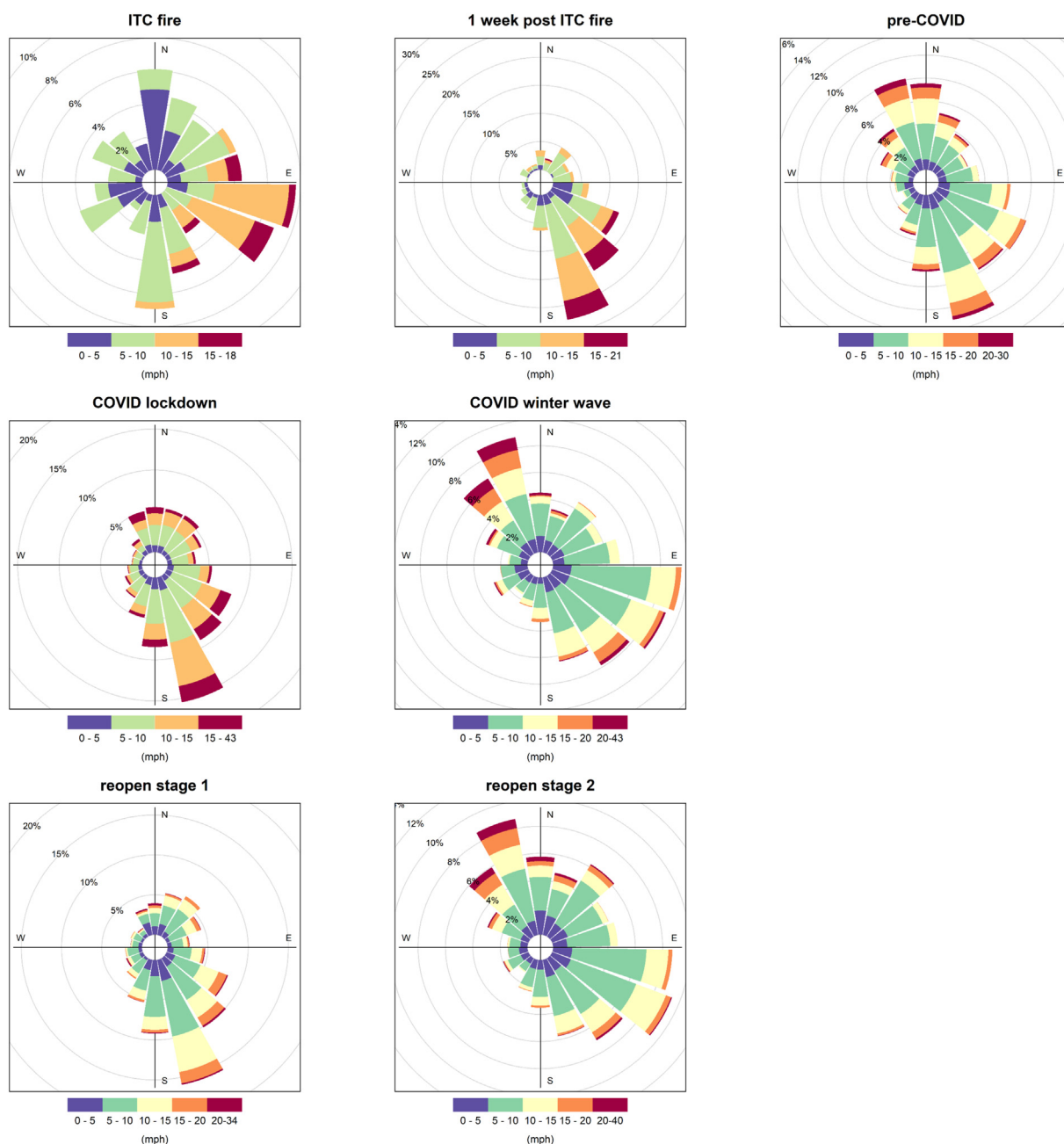


Fig. 2. Windrose plots for ITC fire and COVID periods using weather data measured at Houston Intercontinental Airport.

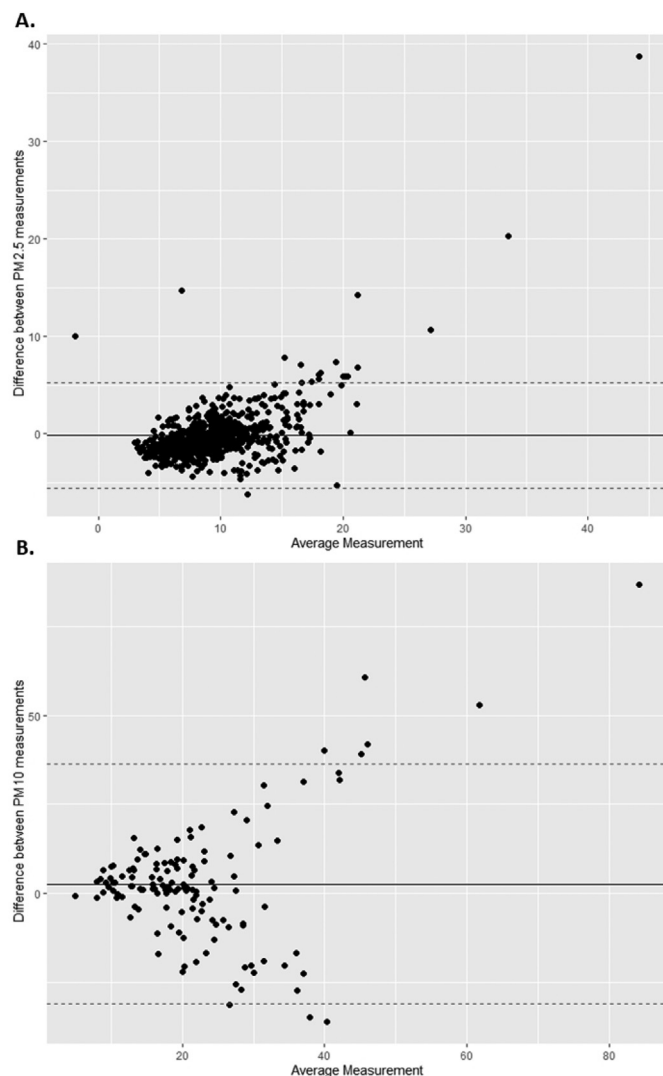


Fig. 3. Bland-Altman plots for the relationship between air pollutions measured by regulatory monitors and low-cost sensor networks.

range from -31.06 to 36.37 for PM_{10} . This suggests that $PM_{2.5}$ data from regulatory monitors were on average 0.18 lower than low-cost sensors, whereas for PM_{10} , regulatory observations were on average 2.65 higher.

3.2. Air pollutions exposure inequality

Fig. 4 shows the distribution of PM_1 between March 2019 to December 2020 and the different environmental justice variables in the region. Higher levels of PM_1 were associated with areas with higher percentages of low-income populations and higher percentages of the population with less than high school education. The distribution of $PM_{2.5}$ was similar to PM_1 (Fig. 5). In areas near major highways with higher percentages of minorities, levels of PM_{10} were higher than in areas with lower percentages of minorities (Fig. 6). For example, along highway I-10, there were seven low-cost sensors. Four of these were in or near areas with a higher proportion of minority populations and showed higher levels of PM_{10} .

In the linear regression between exposure level and census block environmental justice variables, we found that demographic index was significantly associated with PM_1 (β [95 % CI] = $2.93[0.91, 4.95]$), $PM_{2.5}$ (β [95 % CI] = $5.62[1.21, 10.03]$), and PM_{10} (β [95 % CI] = $14.61[4.80, 24.42]$) during pre-COVID, as well as percentage of minority and percentage of low-income population (Table 4). Higher levels of PM_1 and PM_{10} were associated with demographic index and percentage

minority population during and after the ITC fire. Environmental justice variables were associated with higher levels of PM_{10} , compared to PM_1 and $PM_{2.5}$. The percentage of low education and linguistic isolation was not significantly associated with pollutant levels. Using all-time average data, only PM_{10} was consistently associated with environmental justice variables (Table 4).

4. Discussion

In this study, we examined the observations of the low-cost sensor network in the Houston-Harris County area between March 2019 and December 2020, assessing the impact of both an anthropogenic incident (ITC fire) and a natural incident (COVID-19) and the association with the environment inequality. We also conducted a sensitivity analysis comparing the results from low-cost sensors with data collected from the EPA regulatory network.

4.1. Low-cost sensor and regulatory monitoring networks

Our study found that the low-cost sensor network reported comparable $PM_{2.5}$ data to the regulatory network and more robust PM_1 and PM_{10} data with a greater spatial variety and a greater number of hotspots with high pollutants concentration. Concentrations were higher in areas with greater socioeconomic disadvantages. In addition, we observed decreased pollution levels upon the implementation of lockdown restrictions related to the COVID-19 pandemic and 1 week after the ITC fire was extinguished. It is worth noting that, while regulatory monitors were not able to provide data on PM_1 and PM_{10} around the time of the ITC fire, data from low-cost sensors in the surrounding communities nearby Deer Park showed increased levels of pollution during the ITC explosion and immediate decreases one week after the explosion. This suggests that air pollution levels could be underestimated or overlooked without low-cost sensors due to lack of monitoring data in cases of anthropological incidents such as chemical explosions.

The pattern of PM levels detected during and after the ITC fire was similar to that of fire-related incidents. A recent study on the wildfires' contribution to $PM_{2.5}$ levels found that wildfire smoke in the summer could partly account for the increased levels of fine particle pollution in the western US, compared to the seasonal reduction of $PM_{2.5}$ in spring and summer in the eastern US (O'Dell et al., 2019). The study used the trend data from 2006 to 2016, suggesting the impact of wildfires on $PM_{2.5}$ levels was consistent and reoccurring during those years. A study on metropolitan fireworks showed a substantial increase in fine particles and ultrafine particles 24-h after major holidays with fireworks events (Hoyos et al., 2020; Seidel and Birnbaum, 2015). Another example of human-induced disaster is the 2001 World Trade Center Disaster. Study showed $PM_{2.5}$ levels were elevated in the surrounding areas until mid-October (Landrigan et al., 2004). Wind and rain decrease the concentration while thermal inversion increases the concentration. The same mechanism also applies to ITC fire pollutants. Internationally, a study of 23 major industrial fires from the United Kingdom (UK) reported PM behavior similar to what was found in our analysis (Griffiths et al., 2018). The UK study used the UK Air Quality in Major Incidents service network with Osiris laser light scattering monitors and detected incident-average $PM_{2.5}$ levels up to $258 \mu\text{g}/\text{m}^3$ and PM_{10} levels up to $1450 \mu\text{g}/\text{m}^3$. The emission from these incidents could have more significant impacts during seasons with higher background ambient pollution levels or periods where atmospheric conditions inhibit mixing. In our study, $PM_{2.5}$ is the only pollutant measured in both low-cost sensors and the regulatory monitors during the ITC fire. While the average differences between the two monitoring networks were not statistically significant, the mean concentration of $PM_{2.5}$ during the ITC fire was $13.45 \mu\text{g}/\text{m}^3$ from regulatory monitors which is greater than the EPA standard $-12 \mu\text{g}/\text{m}^3$. However, the average concentrations from the low-cost sensor were below the national standard. The precision for low-cost sensors was overall lower than the regulatory network. Low-cost sensors had higher inter- and intra- variance than regulatory monitors with the exception of the

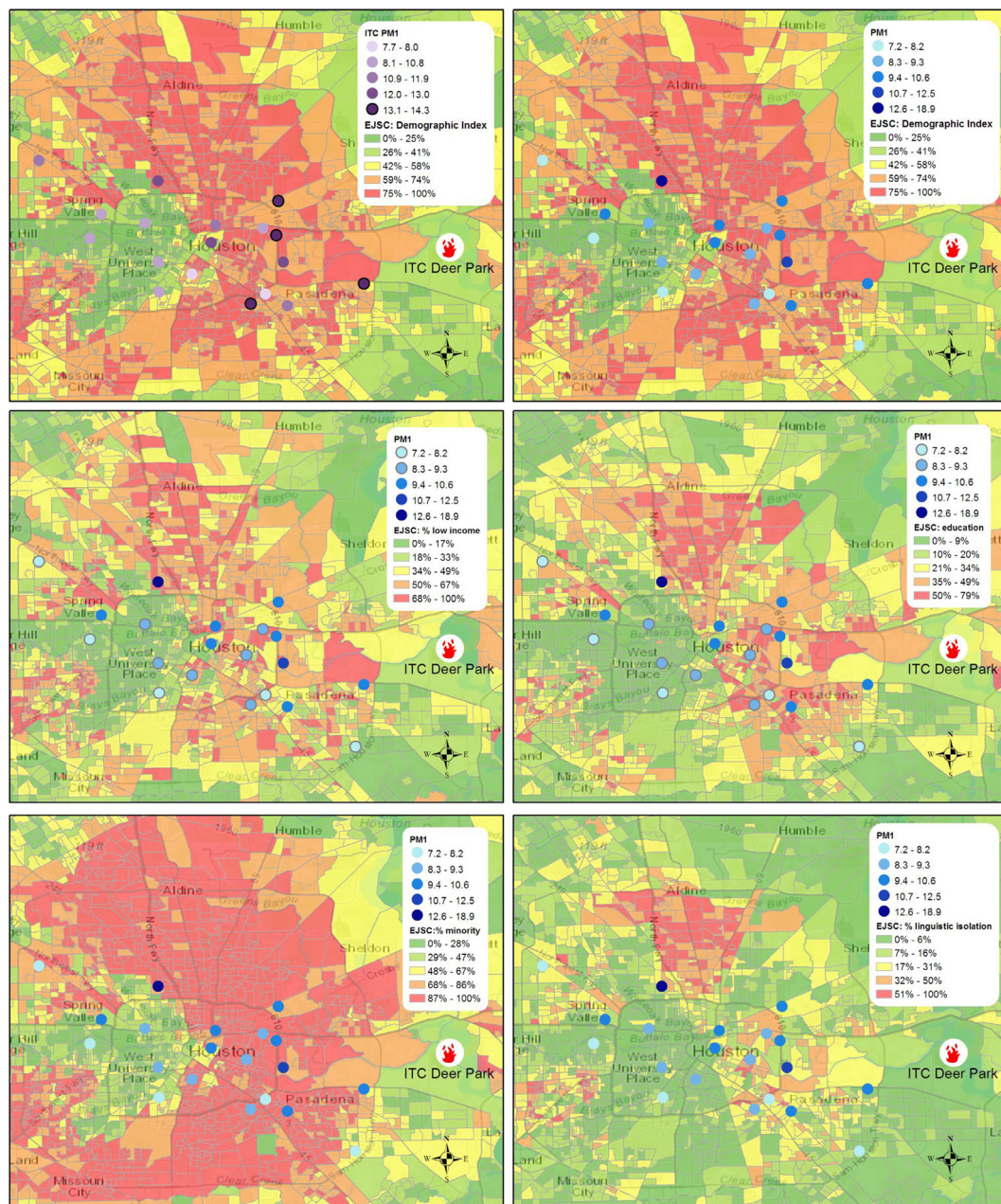


Fig. 4. Maps of PM_{10} concentration with environmental justice factors. (A) ITC PM_{10} levels with demographic index, (B) Average PM_{10} levels with demographic index, (C) Average PM_{10} levels with percentage of low-income population, (D) Average PM_{10} levels with percentage of low-education population, (E) Average PM_{10} levels with percentage of minority population, (F) Average PM_{10} levels with percentage of households in linguistic isolation.

intra-variance for $PM_{2.5}$. These results are expected, as there were a greater number of low-cost sensors than regulatory monitoring sites, resulting in more spatial heterogeneity of monitor locations and a greater number of observations in low-cost sensor network. Previous low-cost sensor studies reported similar results (English et al., 2020). These characteristics of low-cost sensors are also beneficial for public health equality and equity research. For example, a large spatial variation in the network coverage area of various land use, demographic characteristics, and distance to a major highway is beneficial for capturing real-time data in numerous locations with varying socioeconomic conditions, which is useful for conducting environmental justice analyses.

This study found that low-cost sensors provided more comparable data to the regulatory network for $PM_{2.5}$ than PM_{10} over the 1.25 years period. This was partly due to the long interval of PM_{10} data collection from the regulatory network. For $PM_{2.5}$ data, low-cost sensors captured more

extreme value than regulatory monitors. It is unlikely such differences were caused by measurement technological limitations of regulatory monitors, and more likely due to the measurement interval and spatial variation differences, though there is higher uncertainty in the optical particle counter sensors for PM_{10} than $PM_{2.5}$. Previous studies indicated that considerably more episodes of high $PM_{2.5}$ were observed by low-cost sensors compared to regulatory monitors (Seto et al., 2019). While regulatory monitors are geographically located to measure average regional air pollution levels and enforce environmental regulations, the low-cost sensor network can serve many more objectives, including environmental research and neighborhood real-time pollution reports.

In our study, we observed a decrease in $PM_{2.5}$ and PM_{10} concentrations after COVID-19 started in March. Since all of our low-cost sensors were located inside Houston metropolitan area, we were unable to examine differences in the impacts of COVID-19 between urban and rural areas.



Fig. 5. Maps of $PM_{2.5}$ concentration with environmental justice factors. (A) ITC $PM_{2.5}$ levels with demographic index, (B) Average $PM_{2.5}$ levels with demographic index, (C) Average $PM_{2.5}$ levels with percentage of low-income population, (D) Average $PM_{2.5}$ levels with percentage of low-education population, (E) Average $PM_{2.5}$ levels with percentage of minority population, (F) Average $PM_{2.5}$ levels with percentage of households in linguistic isolation.

Previous studies on COVID-19s impact on air pollution suggested $PM_{2.5}$ levels showed a consistent decrease in March 2020 in the urban area compared to the same time period in 2019 (Tanzer-Gruener et al., 2020; Chadwick et al., 2021).

4.2. Environmental disparity in air pollution

Both graphical and statistical examinations showed that, air pollutant levels and environmental justice variables in race and income were highly correlated both during normal conditions and after major anthropogenic or natural incidents in the Houston area. In the ITC fire accident, tanks containing xylene, toluene, gasoline, blendstock, base oil, and naphtha were involved in the direct collision, combustion of which releases hazardous with short-term and long-term exposure. This incident released toxic organic materials and PM into the local and surrounding neighborhoods, causing

public health safety to be compromised in these areas. Work and school activities were canceled in response to the neighborhood concerns of a potential increased outdoor air pollution exposure (Deer Park Emergency Services, 2019). During and after the ITC fire, we found that pollution disproportionately affected the disadvantaged neighborhoods. Levels of PM_1 , $PM_{2.5}$, and PM_{10} were all higher in areas with greater demographic index (higher percentage of minority and low-income population). This emphasized the importance of developing continuous monitoring in these neighborhoods to obtain more accurate estimates of the pollution exposure. The lack of monitoring data limits the research ability to evaluate the impacts of short industrial incidents on health for residents in disadvantaged neighborhoods (Goldman et al., 2021).

The analysis of impacts of the COVID-19 lockdown showed lockdown policies impacted the association between PM and neighborhoods with larger minority populations. This suggests these neighborhoods might be

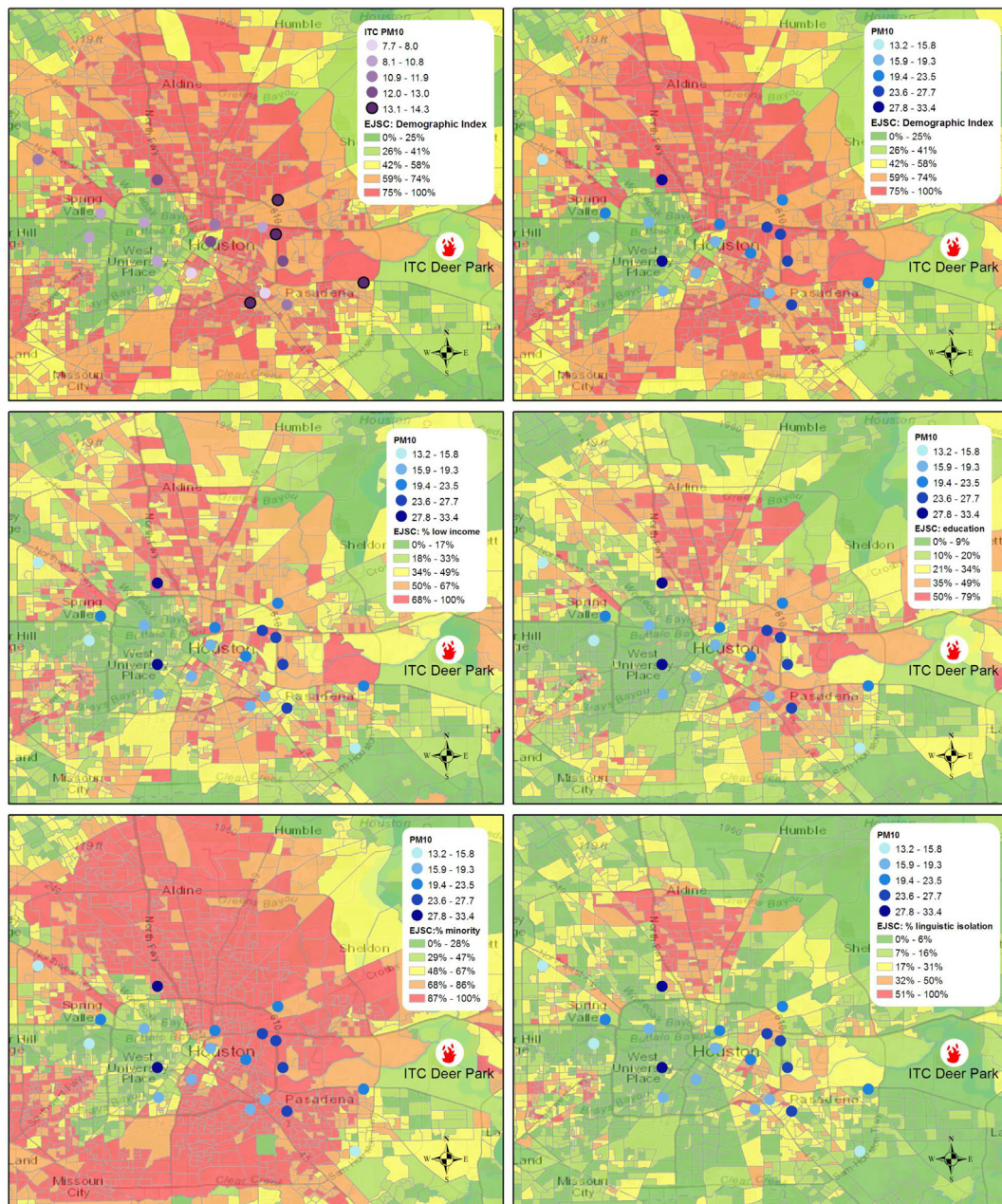


Fig. 6. Maps of PM_{10} concentration with environmental justice factors. (A) ITC PM_{10} levels with demographic index, (B) Average PM_{10} levels with demographic index, (C) Average PM_{10} levels with percentage of low-income population, (D) Average PM_{10} levels with percentage of low-education population, (E) Average PM_{10} levels with percentage of minority population, (F) Average PM_{10} levels with percentage of households in linguistic isolation.

exposed to higher concentrations of traffic-related PM. Our findings ranged from the northwest to southeast of Houston. The distribution of the sensors may bring some bias since it was not evenly distributed around Houston communities. This suggests a need to increase the number of air monitors inside the community to improve our understanding of air pollution disparities and injustice, especially in populated areas including Humble, Fresno and Missouri City. Using low-cost sensors can help measure environmental injustice and provide evidence for public health policy and urban planning. It can also raise awareness in environmental injustice, and collect data for for education purposes, without unbearable costs for local governments, communities, and school districts.

To our knowledge, this is the first study using low-cost sensor observations to examine PM levels during ITC and COVID-19, with a comparison to regulatory air monitors in the Houston area. Previous studies looked into the association between low-cost sensor networks and sociodemographic

factors, but these studies have not examined this in the Houston area. We have reliable PM measurements from the low-cost sensor network over a wide variety of locations. Other benefits of the low-cost sensor network include a faster administrative process when adding new sensors to the low-cost network than the regulatory network and capturing more peak value than regulatory monitors. Some of the disadvantages of utilizing the low-cost sensor network are requirements for ample data storage and processing, sensor hardware maintenance, and software development. It also poses challenges in data sharing and public availability with the current underdeveloped information channels.

5. Conclusion

In this study, we presented the data collected from the low-cost sensor network in the Houston area and examined the impact of ITC fire

Table 4

Linear regression between low-cost sensor observations and environmental justice factors.

Environmental justice factors	Analysis period	PM ₁	PM _{2.5}	PM ₁₀
		β (95 % CI)	β (95 % CI)	β (95 % CI)
Demographic index	all time	3.48(−0.66,7.62)	3.36(−0.14,6.87)*	10.97(3.54,18.40)**
	ITC fire	3.11(−0.12,6.35)*	2.66(−0.96,6.28)	9.47(2.33,16.61)**
	1-week post fire	2.13(−0.23,4.49)*	2.35(−0.29,4.99)*	7.59(2.01,13.17)**
	pre-COVID	2.93(0.91,4.95)**	5.62(1.21,10.03)**	14.61(4.80,24.42)**
	COVID lockdown	1.13(−0.71,2.98)	2.89(−0.55,6.34)	4.60(−1.24,10.44)
	reopen stage 1	1.61(0.11,3.11)*	3.11(0.67,5.55)**	5.01(0.75,9.26)**
	reopen stage 2	2.16(−3.34,7.65)	4.11(−0.80,9.02)	7.44(−6.11,20.98)
	COVID winter wave	2.79(0.04,5.55)*	4.60(0.09,9.11)*	9.63(0.50,18.77)*
Percentage of minority	all time	2.80(−1.30,6.89)	3.36(−0.14,6.87)*	10.97(3.54,18.40)**
	ITC fire	3.58(0.61,6.55)**	2.66(−0.96,6.28)	9.47(2.33,16.61)**
	1-week post fire	2.24(0.00,4.49)*	2.35(−0.29,4.99)*	7.59(2.01,13.17)**
	pre-COVID	2.64(0.65,4.63)**	5.62(1.21,10.03)**	14.61(4.80,24.42)**
	COVID lockdown	1.07(−0.61,2.75)	2.89(−0.55,6.34)	4.60(−1.24,10.44)
	reopen stage 1	1.46(0.09,2.83)*	3.11(0.67,5.55)*	5.01(0.75,9.26)**
	reopen stage 2	1.53(−3.46,6.53)	4.11(−0.80,9.02)**	7.44(−6.11,20.98)
	COVID winter wave	2.28(−0.28,4.83)	4.60(0.09,9.11)	9.63(0.50,18.77)*
Percentage of low income people	all time	3.27(−1.06,7.59)	3.88(0.26,7.51)*	10.97(3.54,18.40)**
	ITC fire	1.80(−1.88,5.48)	2.48(−1.51,6.47)	9.47(2.33,16.61)**
	1-week post fire	1.47(−1.09,4.03)	2.39(−0.42,5.19)	7.59(2.01,13.17)**
	pre-COVID	2.13(0.05,4.21)*	6.71(2.29,11.12)**	14.61(4.80,24.42)**
	COVID lockdown	0.44(−1.61,2.48)	3.65(−0.27,7.57)*	4.60(−1.24,10.44)
	reopen stage 1	1.22(−0.51,2.95)	3.59(0.79,6.38)**	5.01(0.75,9.26)*
	reopen stage 2	2.64(−4.00,9.28)	6.13(0.53,11.73)*	7.44(−6.11,20.98)**
	COVID winter wave	2.69(−0.59,5.97)	6.38(1.28,11.47)**	9.63(0.50,18.77)
Percentage of Lower education people	all time	1.45(−6.57,9.47)	6.49(0.23,12.76)*	8.73(−7.06,24.52)
	ITC fire	4.54(−1.72,10.80)	6.17(−0.31,12.64)*	14.32(0.15,28.50)*
	1-week post fire	2.57(−1.91,7.05)	4.86(0.20,9.52)*	10.72(−0.15,21.59)*
	pre-COVID	2.76(−1.45,6.98)	7.47(−1.07,16.01)	13.68(−6.97,34.33)
	COVID lockdown	−0.05(−3.31,3.21)	4.60(−1.27,10.48)	3.76(−6.68,14.19)
	reopen stage 1	0.46(−2.41,3.32)	4.57(0.24,8.90)*	4.58(−3.45,12.62)
	reopen stage 2	−3.49(−13.13,6.15)	4.05(−5.09,13.18)	−0.84(−25.47,23.79)
	COVID winter wave	2.40(−3.39,8.18)	8.39(−0.19,16.98)*	14.53(−3.70,32.75)
Percentage of people in linguistic isolation	all time	−5.71(−19.09,7.68)	10.60(−0.15,21.35)*	8.73(−7.06,24.52)
	ITC fire	−4.85(−15.71,6.00)	9.75(−1.69,21.20)	14.32(0.15,28.50)*
	1-week post fire	−1.13(−7.77,5.51)	8.37(0.57,16.18)*	10.72(−0.15,21.59)*
	pre-COVID	−0.17(−6.50,6.16)	10.79(−5.58,27.15)	13.68(−6.97,34.33)
	COVID lockdown	−1.16(−6.23,3.91)	10.76(0.11,21.42)*	3.76(−6.68,14.19)
	reopen stage 1	−2.31(−6.69,2.07)	7.94(−0.24,16.12)*	4.58(−3.45,12.62)
	reopen stage 2	−5.68(−22.93,11.58)	10.71(−5.21,26.63)	−0.84(−25.47,23.79)
	COVID winter wave	1.65(−6.67,9.96)	15.75(1.68,29.81)*	14.53(−3.70,32.75)

** $P < 0.05$.* $P < 0.1$.

accident and COVID-19 on air quality in environmental justice communities. We found that observations from a low-cost sensor network were reliable and provided larger spatial coverage and higher temporal resolution to identify hotspots and peak concentrations than regulatory monitoring. Low-cost sensor data also showed environmental justice communities with higher minority and lower socioeconomic status (SES) were exposed to higher pollutant levels. Future low-cost sensor networks in the Houston area should expand further to Houston's low SES communities for community-based monitoring. Low-cost sensors provide critical information for stakeholders and communities to respond to disasters as well as environmental injustice.

CRedit authorship contribution statement

Guning Liu: Conceptualization, Methodology, Visualization, Formal analysis, Writing - original draft. **Katie Moore:** Investigation, Data curation, Writing - original draft. **Wei-Chung Su:** Writing - review & editing. **George L. Delclos:** Writing - review & editing. **David Gimeno Ruiz de Porras:** Writing - review & editing. **Bing Yu:** Writing - review & editing. **Hezhong Tian:** Writing - review & editing. **Bin Luo:** Writing - review & editing. **Shao Lin:** Writing - review & editing. **Grace Tee Lewis:** Data curation, Resources. **Elena Craft:** Conceptualization, Data curation, Funding acquisition. **Kai Zhang:** Conceptualization, Methodology, Supervision, Writing - original draft, Funding acquisition.

Data availability

Data will be made available on request.

Declaration of competing interest

KM is currently employed at a commercial sensor provider (Clarity Movement Co.); this relationship did not affect the work presented here. Other authors declare that they have no known competing financial interests or personal relationships that could have appeared to influence the work reported in this paper.

Acknowledgments

The study was partially supported by Environmental Defense Fund. This paper does not necessarily reflect the views of the Environmental Defense Fund and the University at Albany. WS, GD and DGR were partially funded by the Southwest Center for Occupational and Environmental Health (SWCOEH), a National Institute for Occupational Safety and Health (NIOSH) Education and Research Center at The University of Texas Health Science Center at Houston School of Public Health, and awardee of Grant No. 5T42OH008421 from the NIOSH/Centers for Disease Control and Prevention. The authors appreciate the assistance of Mr. Levi Stanton at Clarity Movement Co. in calibrating the field data.

Availability of data and material

Research data supporting the analysis presented are available upon reasonable request.

Appendix A. Supplementary data

Supplementary data to this article can be found online at <https://doi.org/10.1016/j.scitotenv.2022.157881>.

References

- Air QSPEC-S, 2018. Clarity Sensor Lab Evaluation [PDF]. https://assets.website-files.com/5ef40c2033b60c551ba5c6af/5efab985f324053d86c64d4_clarity-node-lab-evaluation.pdf. (Accessed 24 April 2021).
- Air QSPEC-S, 2018. Clarity Sensor Field Evaluation [PDF]. https://assets.website-files.com/5f64f95d58facb3cb9ddca5b/5f7696ed52371cfee99d672_AQ-SPEC%20Testing%20Report.pdf. (Accessed 24 April 2021).
- Airparif-Airlab, 2018. Airparif & Urban Lab - AIRLAB 2018 microsensor challenge report (French) [PDF]. https://assets.website-files.com/5f64f95d58facb3cb9ddca5b/5f7696af84dee4f614ed7bee_AIRLAB%20Testing%20Results.pdf. (Accessed 24 April 2021).
- American Lung Association, State of the air 2019. www.lung.org/research/sota/key-findings.html. (Accessed 24 April 2019).
- Bechle, M.J., Millet, D.B., Marshall, J.D., 2013. Remote sensing of exposure to NO₂: satellite versus ground-based measurement in a large urban area. *Atmos. Environ.* 69, 345–353.
- Berman, J.D., Ebisu, K., 2020. Changes in US air pollution during the COVID-19 pandemic. *Sci. Total Environ.* 739, 139864.
- Brook, R.D., Rajagopalan, S., Pope III, C.A., Brook, J.R., Bhatnagar, A., Diez-Roux, A.V., Holguin, F., Hong, Y., Luepker, R.V., Mittleman, M.A., 2010. Particulate matter air pollution and cardiovascular disease: an update to the scientific statement from the American Heart Association. *Circulation* 121, 2331–2378.
- California Resources Board. Inhalable Particulate Matter and Health (PM_{2.5} and PM₁₀).
- Chadwick, E., Le, K., Pei, Z., Sayahi, T., Rapp, C., Butterfield, A., Kelly, K., 2021. Understanding the effect of COVID-19 on particle pollution using a low-cost sensor network. *J. Aerosol Sci.* 155, 105766.
- Clarity, M.C., .. Node-S Technical Specifications [PDF]. https://click.clarity.io/hubfs/Marketing%20Assets%20-%20PDFs/Product%20and%20Specification%20Sheets/Node%20S%20Specifications%20Sheet.pdf?_ga=2.107630466.1601822225.1646802589-217804954.1646689543. (Accessed 24 April 2021).
- Deer Park Emergency Services, 2019. ITC Fire Updates. Deer Park Emergency Services. <http://www.deerparktx.gov/1778/ITC-Fire>. (Accessed 10 August 2022).
- English, P., Amato, H., Bejarano, E., Carvlin, G., Lugo, H., Jerrett, M., King, G., Madrigal, D., Meltzer, D., Northcross, A., 2020. Performance of a low-cost sensor community air monitoring network in imperial county, CA. *Sensors* 20, 3031.
- European Environment Agency, 2020. Air Pollution Goes Down as Europe Takes Hard Measures to Combat Coronavirus. EEA News. <https://www.eea.europa.eu/highlights/air-pollution-goes-down-as>. (Accessed 10 August 2022).
- Fu, P., Guo, X., Cheung, F.M.H., Yung, K.K.L., 2019. The association between PM_{2.5} exposure and neurological disorders: a systematic review and meta-analysis. *Sci. Total Environ.* 655, 1240–1248.
- Gautam, S., 2020. COVID-19: air pollution remains low as people stay at home. *Air Qual. Atmos. Health* 13, 853–857.
- Goldman, G.T., Desikan, A., Morse, R., Kalman, C., MacKinney, T., Cohan, D.S., Reed, G., Parras, J., 2021. Assessment of air pollution impacts and monitoring data limitations of a spring 2019 chemical facility fire. *Environ. Justice* <https://doi.org/10.1089/env.2021.0030>.
- Griffiths, S.D., Chappell, P., Entwistle, J.A., Kelly, F.J., Deary, M.E., 2018. A study of particulate emissions during 23 major industrial fires: implications for human health. *Environ. Int.* 112, 310–323.
- Han, H.A., Han, I., McCurdy, S., Whitworth, K., Delclos, G., Rammah, A., Symanski, E., 2020. The intercontinental terminals chemical fire study: a rapid response to an industrial disaster to address resident concerns in deer park, Texas. *Int. J. Environ. Res. Public Health* 17, 986.
- Hao, Y., Balluz, L., Strosnider, H., Wen, X.J., Li, C., Qualters, J.R., 2015. Ozone, fine particulate matter, and chronic lower respiratory disease mortality in the United States. *Am. J. Respir. Crit. Care Med.* 192, 337–341.
- Hoyos, C.D., Herrera-Mejía, L., Roldán-Henao, N., Isaza, A., 2020. Effects of fireworks on particulate matter concentration in a narrow valley: the case of the Medellín metropolitan area. *Environ. Monit. Assess.* 192, 1–31.
- Krall, J.R., Mulholland, J.A., Russell, A.G., Balachandran, S., Winquist, A., Tolbert, P.E., Waller, L.A., Sarnat, S.E., 2017. Associations between source-specific fine particulate matter and emergency department visits for respiratory disease in four US cities. *Environ. Health Perspect.* 125, 97–103.
- Landrigan, P.J., Lioy, P.J., Thurston, G., Berkowitz, G., Chen, L., Chillrud, S.N., Gavett, S.H., Georgopoulos, P.G., Geyh, A.S., Levin, S., 2004. Health and environmental consequences of the world trade center disaster. *Environ. Health Perspect.* 112, 731–739.
- Liu, S., Zhang, K., 2015. Fine particulate matter components and mortality in greater Houston: did the risk reduce from 2000 to 2011? *Sci. Total Environ.* 538, 162–168.
- Mousavi, A., Wu, J., 2021. Indoor-generated PM_{2.5} during COVID-19 shutdowns across California: application of the PurpleAir indoor-outdoor low-cost sensor network. *Environ. Sci. Technol.* 55, 5648–5656.
- O'Dell, K., Ford, B., Fischer, E.V., Pierce, J.R., 2019. Contribution of wildland-fire smoke to US PM_{2.5} and its influence on recent trends. *Environ. Sci. Technol.* 53, 1797–1804.
- Patel, K., 2020. Airborne Nitrogen Dioxide Plummets Over China.
- Rossi, R., Ceccato, R., Gastaldi, M., 2020. Effect of road traffic on air pollution. Experimental evidence from COVID-19 lockdown. *Sustainability* 12, 8984.
- San JV-APCD, 2018. SJVAPCD - preliminary TEST program evaluation [PDF]. https://assets.website-files.com/5f64f95d58facb3cb9ddca5b/5f7696266ebd2b48b302d37d_SJVAPCD%20Testing%20Report.pdf. (Accessed 24 April 2021).
- Seidel, D.J., Birnbaum, A.N., 2015. Effects of Independence day fireworks on atmospheric concentrations of fine particulate matter in the United States. *Atmos. Environ.* 115, 192–198.
- Seto, E., Carvlin, G., Austin, E., Shirai, J., Bejarano, E., Lugo, H., Olmedo, L., Calderas, A., Jerrett, M., King, G., 2019. Next-generation community air quality sensors for identifying air pollution episodes. *Int. J. Environ. Res. Public Health* 16, 3268.
- Tanzer-Gruener, R., Li, J., Eilenberg, S.R., Robinson, A.L., Presto, A.A., 2020. Impacts of modifiable factors on ambient air pollution: a case study of COVID-19 shutdowns. *Environ. Sci. Technol. Lett.* 7, 554–559.
- Texas Commission on Environmental Quality, 2020. Intercontinental Terminal Company Fire Response (2019)- after action review report. www.tceq.texas.gov/assets/public/response/smoke/air/final-ITC-Fire-AAR-01.07.2020.pdf. (Accessed 24 April 2021).
- United States, .. Environment Protection Agency. "National air toxics assessment 2014". www.epa.gov/sites/default/files/2020-07/documents/nata_2014_summary_of_results.pdf. (Accessed 24 April 2014).
- Wang, P., Chen, K., Zhu, S., Wang, P., Zhang, H., 2020. Severe air pollution events not avoided by reduced anthropogenic activities during COVID-19 outbreak. *Resour. Conserv. Recycl.* 158, 104814.
- World Health Organization, .. Ambient (outdoor) air pollution. [www.who.int/news-room/fact-sheets/detail/ambient-\(outdoor\)-air-quality-and-health](http://www.who.int/news-room/fact-sheets/detail/ambient-(outdoor)-air-quality-and-health). (Accessed 24 April 2021).
- Yang, M., Chu, C., Bloom, M.S., Li, S., Chen, G., Heinrich, J., Markevych, I., Knibbs, L.D., Bowatte, G., Dharmage, S.C., 2018. Is smaller worse? New insights about associations of PM₁ and respiratory health in children and adolescents. *Environ. Int.* 120, 516–524.
- Younan, D., Petkus, A.J., Widaman, K.F., Wang, X., Casanova, R., Espeland, M.A., Gatz, M., Henderson, V.W., Manson, J.E., Rapp, S.R., 2020. Particulate matter and episodic memory decline mediated by early neuroanatomic biomarkers of Alzheimer's disease. *Brain* 143, 289–302.